SSRG International Journal of Electronics and Communication Engineering
ISSN: 2348-8549/ https://doi.org/10.14445/23488549/IJECE-V11I10P114

Volume 11 Issue 10, 176-185, October 2024

Original Article

Analysis of Coupled Waveguide with Multiple Radiation Slots

Joginaidu K[1], Sunny Dayal P. A[2], Raju G. S. N[3]

[1,2,3]*Department of Electronics and Communication Engineering, Centurion University of Technology and Management, Andhra Pradesh, India.*

[1]*Corresponding Author : joginaiduk@outlook.com*

Received: 14 August 2024 Revised: 15 September 2024 Accepted: 14 October 2024 Published: 30 October 2024

Abstract - *Waveguide slot array antennas have unique qualities that make them superior to microstrip antennas in terms of loss and simpler in terms of structure than reflector antennas. As a result, they are widely employed for high-gain flat antennas in wave wireless communication systems. In order to create a slotted waveguide array or waveguide array with longitudinal shunt slots, a precise mutual coupling is necessary. SWG waveguides are used in particle trapping because of their superior bulk and surface sensitivity and their longer working distance compared to conventional nanophotonic waveguides. Furthermore, due to the requirements of basic pharmacological research and biological heterogeneity, parallel trapping of many particles is quite practicable. Furthermore, Sub Wavelength Grating (SWG) waveguides have a longer working distance, allowing for increased particle trapping and Bloch mode-induced optical forces propagation along SWG waveguides. Slotted Waveguide (SWG) array has the advantage of array configuration blended with slot reduction. This work proposes two configurations of slotted waveguides excited by an energy coupled through a primary waveguide. Two array configurations with four and eight slots were simulated, successfully developed, and examined regarding the Voltage Standing Wave Ratio (VSWR), reflection coefficient,3D and 2D radiation patterns, and distant field distribution plots. The significant impact on the Beamwidth (BW) is also investigated.*

Keywords - *Slotted waveguide, Slot array, Coupling slot, Radiation pattern, Beamwidth.*

1. Introduction

Parallel-plate slot array antennas are now popular choices, particularly in the centimetre and millimetre-wave bands, due to their inherent benefits of high gain, high antenna radiation efficiency, low losses, compact structure, and high-power capabilities. These properties make them appropriate for a variety of applications. Compared to the commonly used planar slotted array antenna configuration, which consists of an array of juxtaposed waveguides under single-mode operation with a proper feeding circuit beneath or distribution networks at the same layer, the suppression of the inner sidewalls eliminates the necessity of a minimum distance between radiating elements, making the slot array design more flexible. Nevertheless, due to numerous unknowns, parallel plate antenna analysis software calculations are time-consuming and require careful consideration of the slots' reciprocal connectivity. Emitting and coupling slots are included in slotted waveguides (SWGs). Coupling slots transfer energy from one region to another. A prior design method, which worked with arrays of longitudinal slots supplied by a rectangular waveguide filled with air, is expanded to accommodate the more prevalent practical scenario in which the waveguide is dielectrically filled [1]. To achieve improved array performance, characterized by reduced sidelobe levels and enhanced input matching, approximations are utilized. Techniques must be eliminated from previous designs. One major change is the implementation of internal higher-order mode coupling [2]. The response integral between one slot's field and another slot's corresponding current distribution is directly correlated with the coupling coefficient [3]. A coupling junction is often made up of two longitudinal radiating slots in the branch waveguide that are straddling and spaced one-fourth of the guiding wavelength apart, as well as two cantered-inclined connection slots in two orthogonal waveguides' common broad wall [4]. A slot array groove gap waveguide antenna with the necessary sidelobe level and excellent impedance matching can be designed and completed quickly through the use of analytical formulae.

The construction of a slot array groove gap waveguide antenna with very excellent impedance matching and the necessary sidelobe level can be completed quickly through the use of analytical formulae.

2. Literature Survey

Katehi et al. [5] have proposed that the method uses an integral equation formulation to evaluate slot properties such as self-admittance and resonant frequency. Rengarajan et al. [6] have suggested that the radiating energy into the empty space is similarly caused by the radiating slots. The slotted WG has the obvious advantage of being lighter due to the slots. Jossefson et al. [7] have described that the WG can be both resonant and non-resonant. In general, power loss is inherent with non-resonant waves because they are traveling waves. Oliner et al. [8] have reported that slot location is a major source of contention, as it is also responsible for the WG's frequency-dependent features. Halsall et al. [9] have recommended that the complexity increases with multiple-slot WGs, particularly because the space between the slots has a major effect on the resonance characteristics of the WG. Marshall et al. [10] have reported that the array layout of the slot has no effect on the total slotted WG length because all of the slots are typically organized in an axial line along the longer side of the WG. This is not a general case in linear arrays; thus, it can be regarded as an advantage.

There are several computational methods and strategies proposed by many elites in the field Perovic et al. [11]. Tai et al. [12] have proposed a couple of relations that are required to solve in order to arrive at the position of the slots and the corresponding dimensions of the slots. Oliner et al. [8] have reported that these mathematical relations are directly derived along with formulation to determine the dimension of the slot. The slots can be arranged or displaced uniformly along the length. However, it is possible to control the radiation characteristics of the WG.

In this paper, the slots are uniformly displaced from each other. However, the analysis based on the number of slots has been carried out. The simulations are performed using an efficient electromagnetic simulation tool.

Further, the paper is organized to discuss the geometry in section 2, following the discussion on results in section 3 and overall conclusions in section 4.

3. Proposed System
3.1. Antenna Design

This paper revisits the slotted waveguide architecture, intending to analyze its coupling characteristics. Accordingly, a primary and secondary waveguide is used for the purpose; the primary WG is excited, which does not radiate. However, the secondary WG is the radiating element. For the purpose of coupling and radiation, several slots are arranged on primary and secondary WG, respectively. The typical slot has considerable width and length, resonating with the system's operating frequency.

The primary WG acts as the source; its overall dimensions are 130 x 65 x 32 mm3; the waveguide's thickness is 2 mm. The slot is inclined at an angle of 450 with length and widths of 45 mm and 0.5 mm, respectively. The designed WG is shown in Figure 1. The slot is arranged on the broad surface by removing a conductor strip with some inclination angle, as shown in Figure 1.

Further, the secondary WG has multiple slots on one of the broadsides, while a single slot in compliance with the primary WG is arranged. This single slot is called the coupling slot while the multiple slots are referred to as resonant slots. The couple slot couples the energy from the primary to the secondary while the energy coupled into the secondary is radiated with the help of radiating slots. The overall dimensions of the 4-slot WG are 276 x 69 x 32 mm3. The slot measures 48 mm in length and 0.7 mm in width. The 8-slot WG is 552 x 69 x 32 mm3 in total. The WG has a thickness of 2 mm.

The coupling slot is arranged at a position described as a halfwave point at the centre of the WG with 450 inclination that can provide maximum coupling. However, the radiating slots are arranged on the outer surface of the secondary along with the axial line of the WG. The slots are distributed on either side of the axial line symmetrically. Table 1 displays a performance comparison of several types of antennas.

Table 1. Performance comparison of various types of antennas

Antenna Type	Total Volume w/ Ground Plane (λ_0^3)	Radiation Efficiency (%)	Peak Realized Gain (dBi)
Ref. Patch	1.08×1.08×0.02	86	7.4
Type-A	1.08×1.08×0.02	91	7.6
Type-B	1.08×1.08×0.05	98	8.8
Type-C	1.08×1.08×0.05	98	9.2

3.2. Design and Analysis of the Suggested Antenna Structure

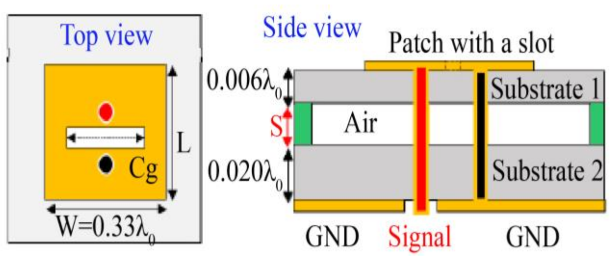

Fig. 1 The proposed prototype with the multi-radiation slots configuration design parameters

The structural development of the proposed antenna from the conventional patch shape is depicted in Figure 1. Configure the Type-A by adding a slot, using a standard patch antenna as a guide, and loading a shorting pin on the reference structure. Additionally, an air-gap structure has a bottom substrate with a slot-loaded patch on the upper substrate and a Type-B ground plane. The connections of the shorting pin and signal are separated by air. Finally, in order to reduce the air-gap profile as much as feasible, the proposed construction is an evolution of the Type-B. It incorporates two symmetric rectangular slots across the middle slot. Matching pads that are vertically loaded are incorporated into the middle levels of the suggested arrangement in order to stabilize the gain characteristics better.

The purpose of these low-profile spacers is to create the air gap between two dielectric substrates totaling four layers. The top layer is composed of a multi-slot loaded patch antenna. layers two and three are made up of two matching pads each. The ground plane is the final component of layer 4. For higher radiation efficiency, Type-A microstrip patch antenna construction is the most commonly used type.

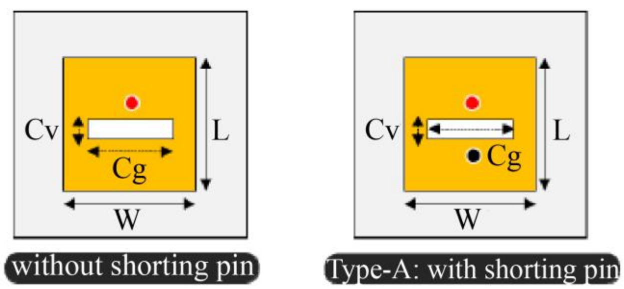

Fig. 2 Shorting pin patch and slotted patch structures with the impact of slot size variation

Figure 2 shows the structure for both slotted and shorting pin patches and the effects of changing the slot size.

3.2.1. Sub-Wavelength Gratings

The wavelength of light incident on a periodic grating (see Figure 3) has a wavelength that depends on the grating period (Λ). This wavelength determines how light propagates k-direction or perpendicular to the layers.

Greater design flexibility is available in this last regime, where the grating transforms into a SWG. While good modeling requires full consideration of the structure close to the bandgap, An anisotropic refractive index can be used to depict the grating as a homogenous material at longer wavelengths (λ ≳ v) tensor$\boldsymbol{n_{SWG}}$:

$$n_{SWG}^2 = \begin{matrix} n_{||}^2 & 0 & 0 \\ 0 & n_{||}^2 & 0 \\ 0 & 0 & n_{||}^2 \end{matrix} \quad (1)$$

Polarizations parallel to grating interfaces (n||) and perpendicular to them (n⊥) have different indices and unique quality of SWGs that have led to their widespread use at NIR wavelengths in a variety of literature; for examples of SWG device implementations in the NIR range, readers are directed to earlier reviews.

For designers of devices, it is crucial to note that the SWG feature sizes, a and Γa (corresponding to n1 and n2, respectively), set a strict restriction on how much flexibility is available for the grating design in terms of being easily manufactured with standard current lithography methods. Additionally, when integrated photonic devices advance to longer MIR wavelengths, thicker waveguiding layers will be required, creating new manufacturing challenges, even though the grating period can extend substantially (easing the lithographic limitation). Producing large aspect ratio features with a uniform etch profile is a tough task, and issues like aspect ratio-dependent etching carry substantial consequences [13]. SWGs can quickly depart from their intended performance because they are especially vulnerable to fabrication mistakes caused by under-etched material within the grating. The authors are unaware of any examples of SWG devices being used in integrated photonic circuits with germanium layers thicker than 1 μm [14].

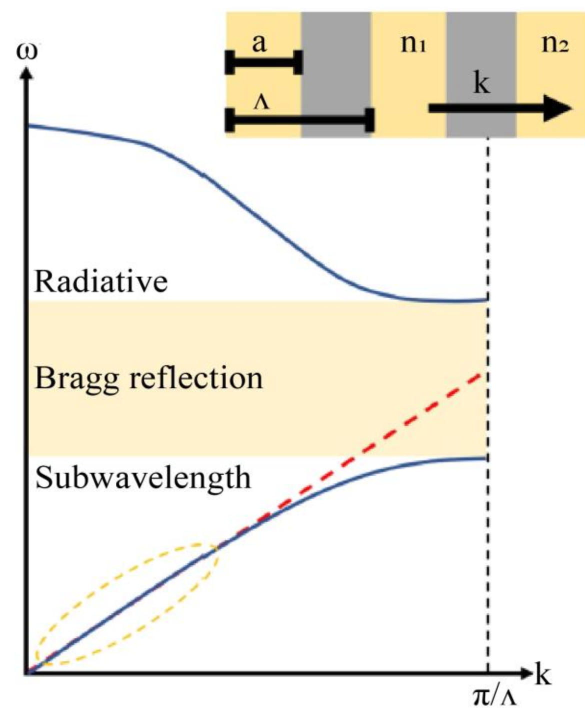

Fig. 3 Illustration of the band structure of a one-dimensional grating with period Λ

3.2.2. Coupling in Radiation Slot Antenna

The length and number of slots in the recommended design's cell structure are adjustable in the X and Y directions, respectively, as illustrated in Figure 4. Nevertheless, more patches will be required for each slot as the length of the slot increases. As a result, the explanations provided below can be applied to any large planar slot array. As shown in Figure 2, the radiation slot antenna connection is seen from both the top and side perspectives. Each slot is fed by a and placed in the center. Figure 4 illustrates how each slot is connected to several rectangular parasitic patches.

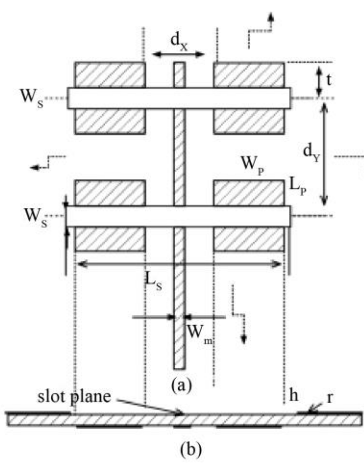

Fig. 4 Coupling in radiation slot antenna: (a) Top view, and (b) Side view.

On the same side of the microstrip feed line as the patches, printing occurs. The length and frequency of operation of two slots influence the number of patches and their distance apart. When considering a typical impedance of 50 Ω, the width W_m of the microstrip when selecting a feed line, the tuning length is less than 0.25 λ_g to match impedances.

A standing wave distribution appears to be formed by positive and negative nodes along the slot electric field's axis perpendicular to the slot length. After propagating for half a wavelength, this electric field's orientation is reversed. This looks to provide a way to produce good front radiation. The negative peak voltage should be located elsewhere if we assume that the positive centre of the slot experiences the highest voltage. By moving the patch along the axis, the patch centre can be moved toward the negative peak voltage, in contrast, giving an intermediate half-wavelength patch, which results in an extremely low input impedance. The high impedance Z_0 of the slot, the line should be effectively shortened by this.

4. Results and Discussion

The antenna is expected to function within a frequency range of roughly 3.27 GHz for the purposes of the study reported here. The slot line's effective length is around 1.5 wavelengths, ensuring the peak voltage is located in the slot's centre. It may be necessary to alter some parameters due to their interactions to achieve the desired antenna performance.

4.1. Case 1

Figure 5(a) depicts the WG's straightforward single-slot architecture. The reflection coefficient and VSWR are used to assess the corresponding features. Figure 5(b) depicts the corresponding S11 plot. Figure 5(c) provides the matching VSWR.

The resonant characteristics are evident from the S11 plot, in which the resonant frequency was identified as 3.27 GHz with an excellent wideband feature. Further, the same is evident from the corresponding VSWR plot given in Figure 5(c), where the curve has shown its minimum value at 3.27 GHz.

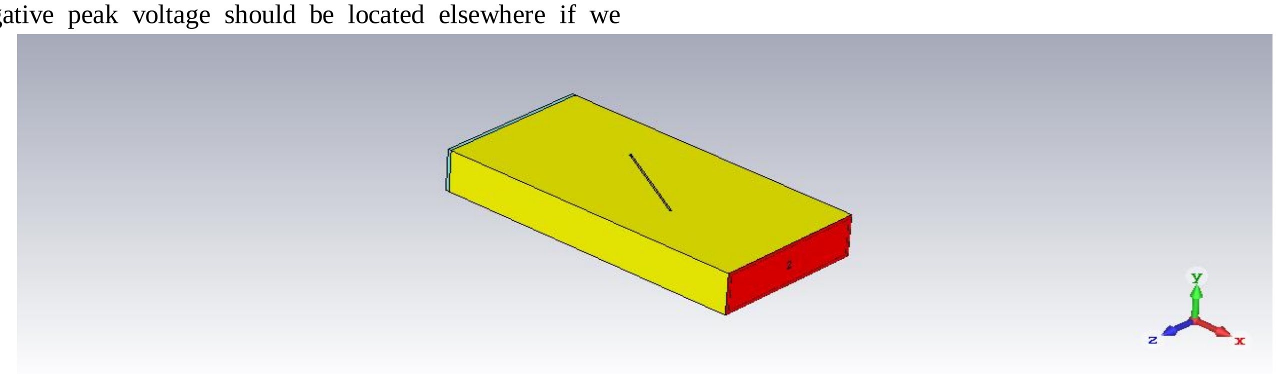

(a)

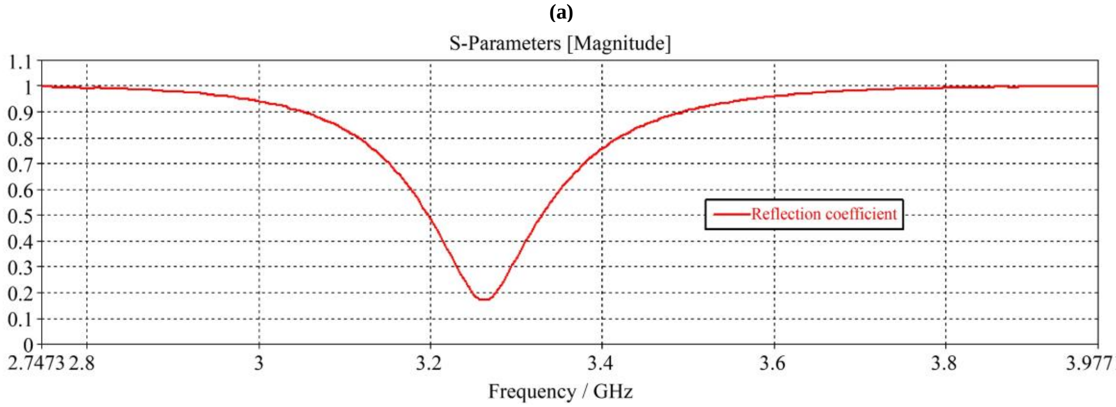

(b)

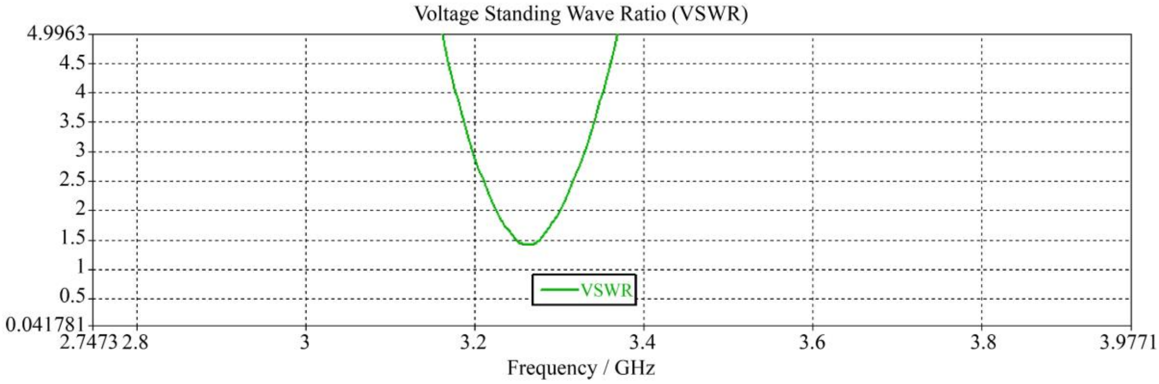

(c)

Fig. 5 WG with the single slot is a representation of (a) WG with a single slot Design, (b) WG with a single slot in the S11 plot, and (C) WG with a single slot representation VSWR plot.

4.2. Case 2

In this case, a four slotted WG (4SWG) is designed, simulated and analyzed based on the structure developed in case 1. Four slots are symmetrically arranged along the centre of the WG. However, in this case, the WG is not excited directly. At the same time, it is coupled with energy from a primary WG, which is excited accordingly. The primary slot is coupling the energy into the secondary WG, which radiates through the slots on the wide dimension. The S11 and the VSWR are studied with the help of Figures 6(b) and 6(c).

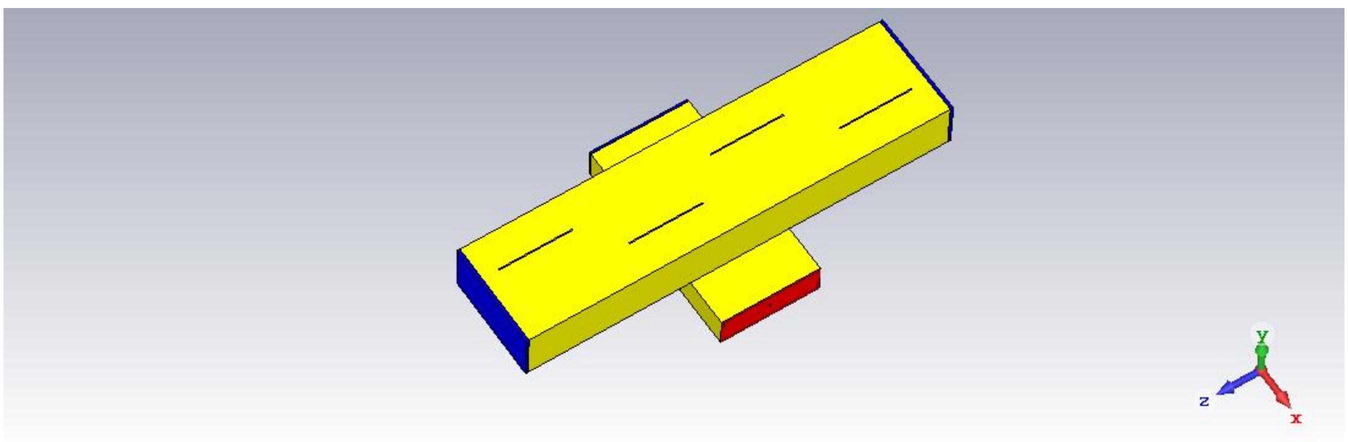

(a)

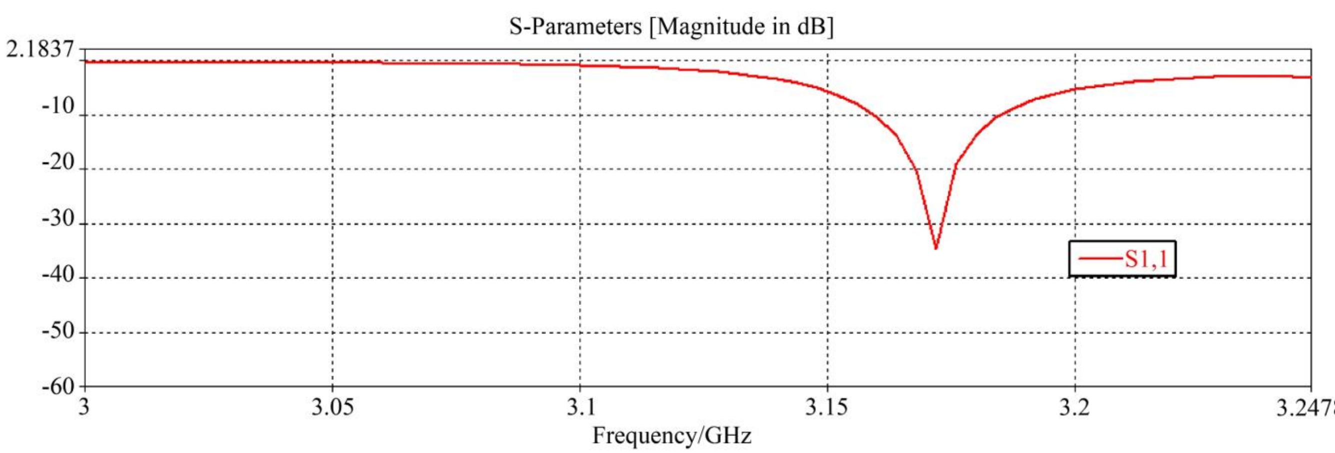

(b)

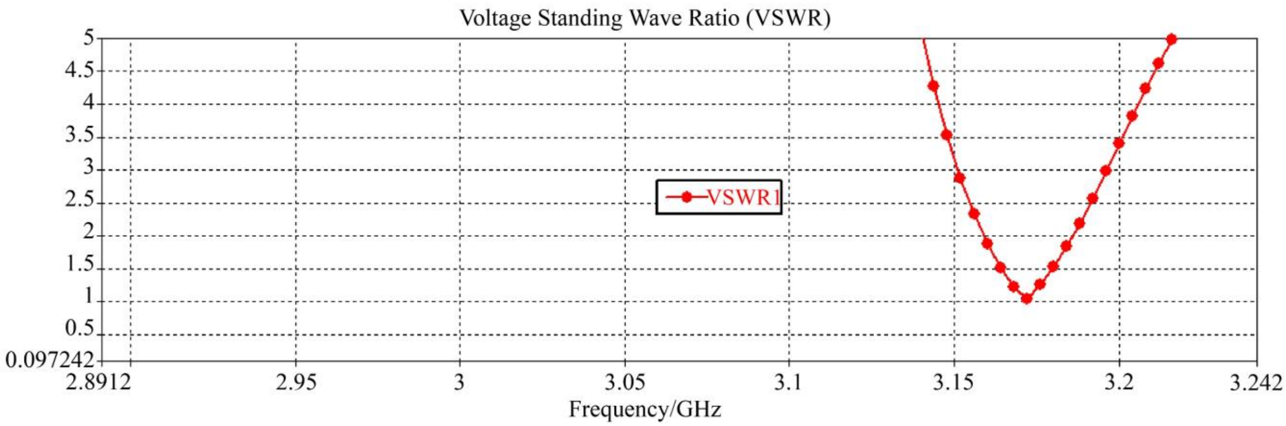

(c)

Fig. 6 The WG flowchart with four slots (4SWG) (a) Four slotted WG (4SWG) design, (b) Four slotted WG (4SWG) S11 plot, and (c) Four slotted WG (4SWG) VSWR plot.

It is possible to mention that the resonant frequency is slightly oriented between 3.15 GHz to 3.2 GHz, showing a consistent S11 below -10 dB and VSWR below '2'.

The field distribution can be viewed with the help of the plot given in Figure 7(a). The concentration can be seen through the region around the slot, diminishing as it reaches the ends of the WG.

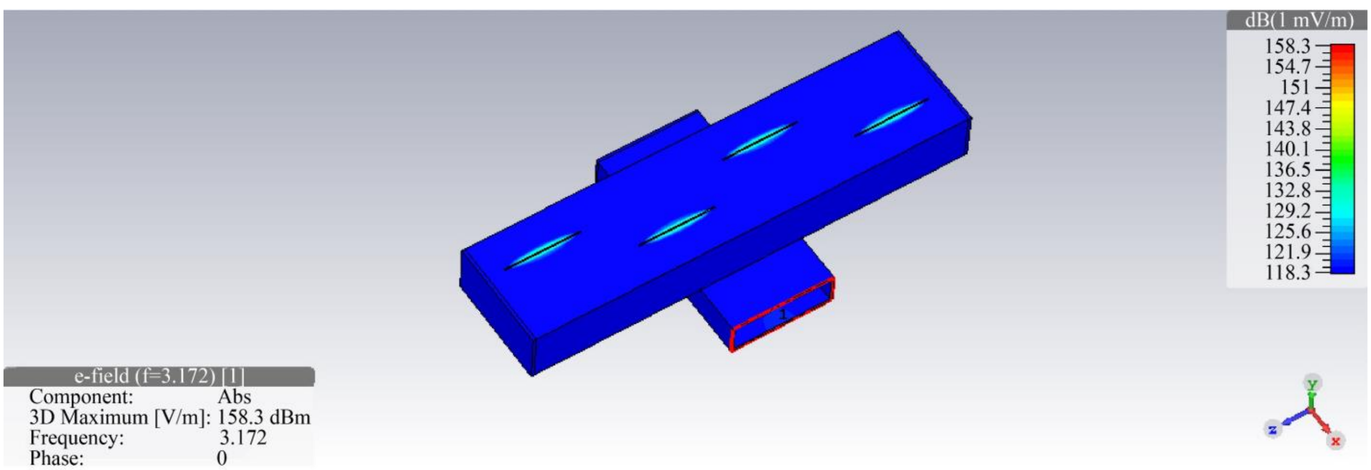

(a)

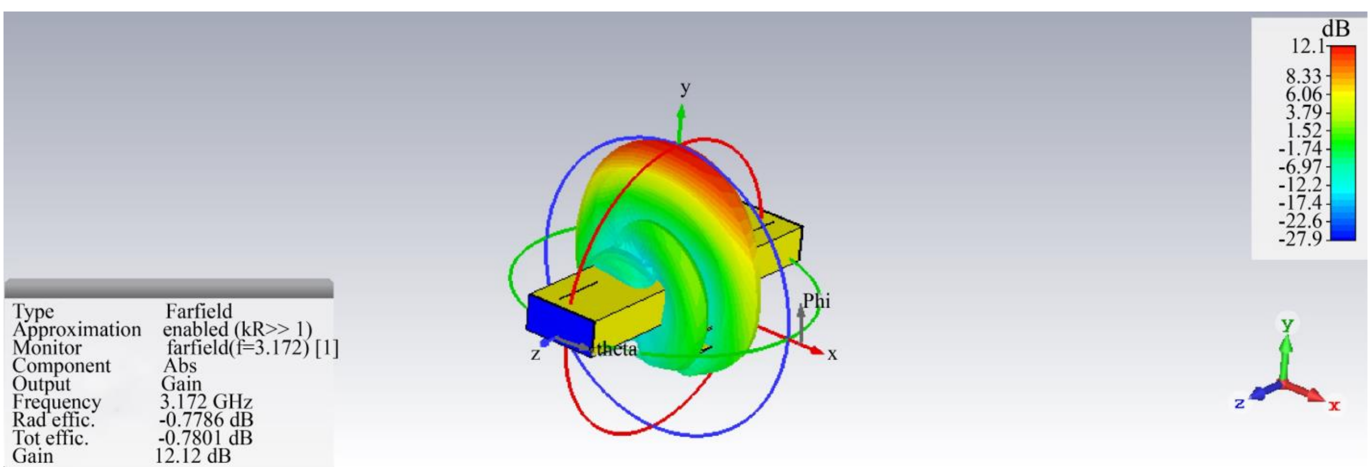

(b)

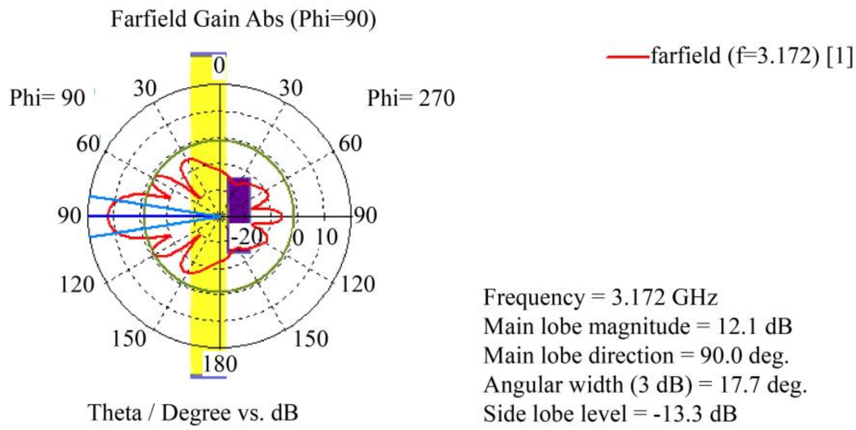

(c)

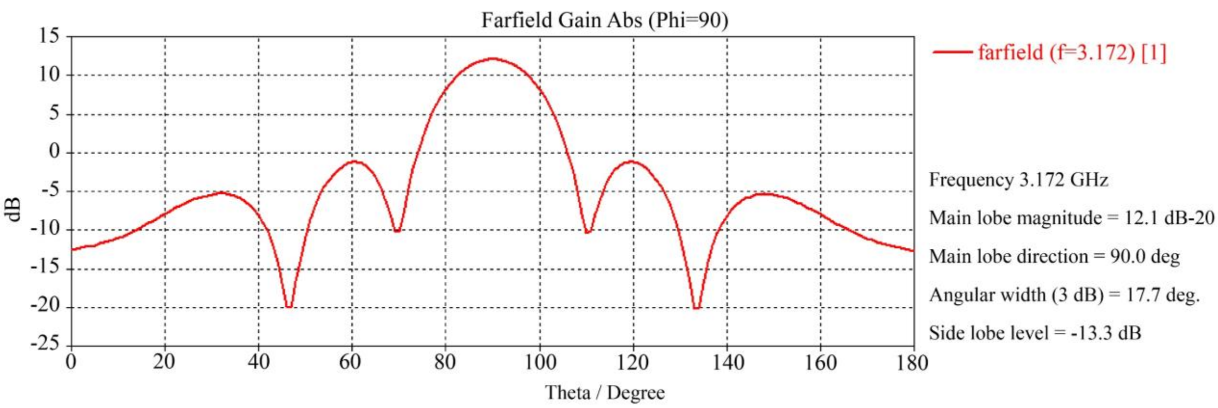

(d)

Fig. 7 4 SWG simulation results (a) E-field distribution, (b) Far-field, (c) Radiation pattern, and (d) Gain plot.

The radiation pattern has a dense region forming the main beam and extending into the far field from the slot. This can analyze using the far-field pattern across the slots, as shown in Figure 7(b). It is possible to have a directional pattern by which the radiation is concentrated only in one direction or one hemisphere. This characteristic type is evident from Figure 7(c), which depicts a polar 2D pattern. According to the plot, the radiation is concentrated through one hemisphere, providing a highly directional characteristic.For better understanding, the gain characteristics are plotted in Figure 7(d), from which the corresponding beam width and the main beam placement are read directly.

4.3. Case 3

8-slot waveguide (8-SWG)

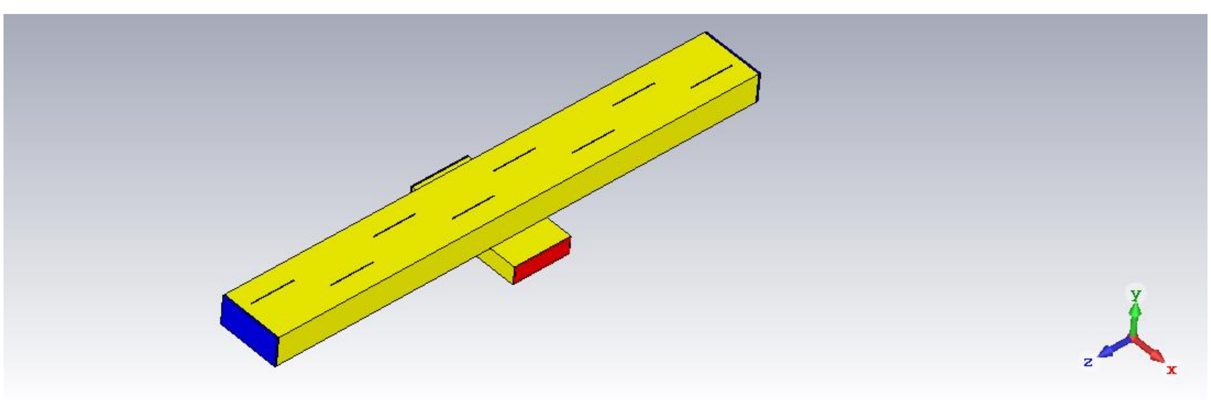

(a)

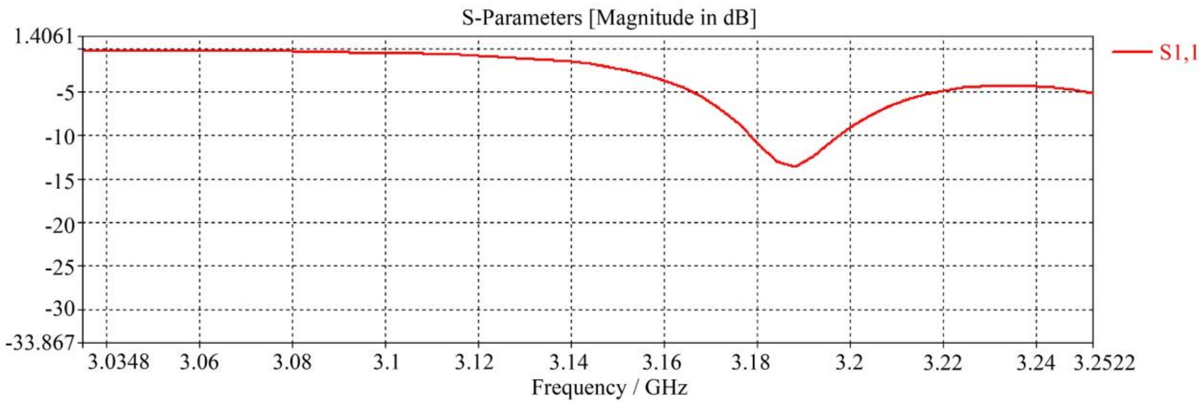
S-Parameters [Magnitude in dB]
S1,1
1.4061
-5
-10
-15
-20
-25
-30
-33.867
3.0348 3.06 3.08 3.1 3.12 3.14 3.16 3.18 3.2 3.22 3.24 3.2522
Frequency / GHz

(b)

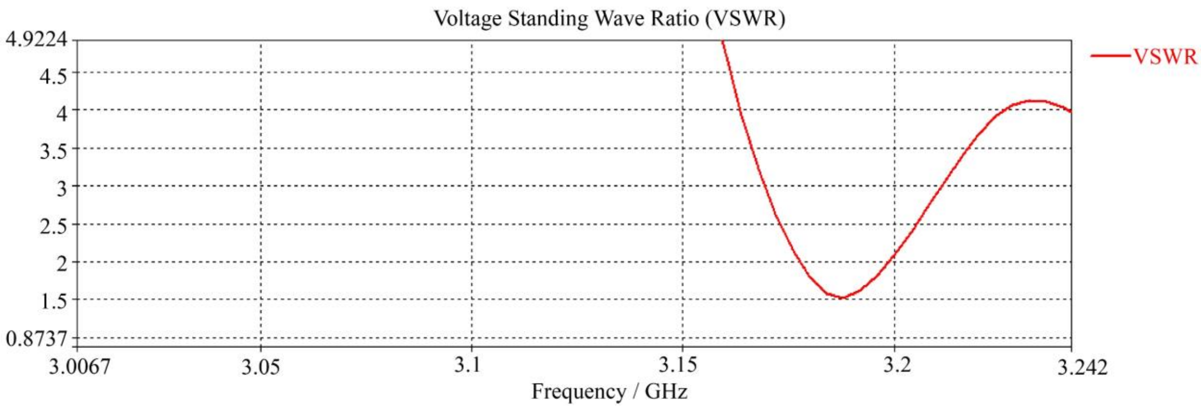
Voltage Standing Wave Ratio (VSWR)
VSWR1
4.9224
4.5
4
3.5
3
2.5
2
1.5
0.8737
3.0067 3.05 3.1 3.15 3.2 3.242
Frequency / GHz

(c)

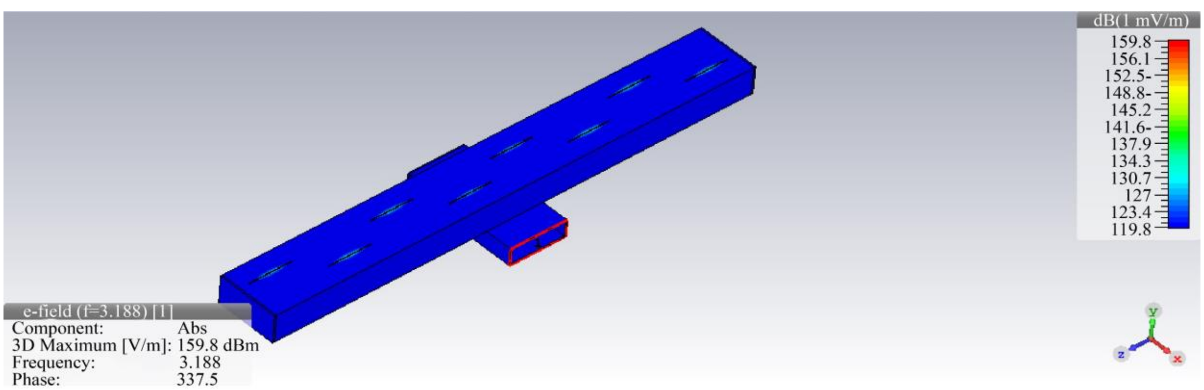
dB(1 mV/m)
159.8
156.1
152.5
148.8
145.2
141.6
137.9
134.3
130.7
127
123.4
119.8
e-field (f=3.188) [1]
Component: Abs
3D Maximum [V/m]: 159.8 dBm
Frequency: 3.188
Phase: 337.5

(d)

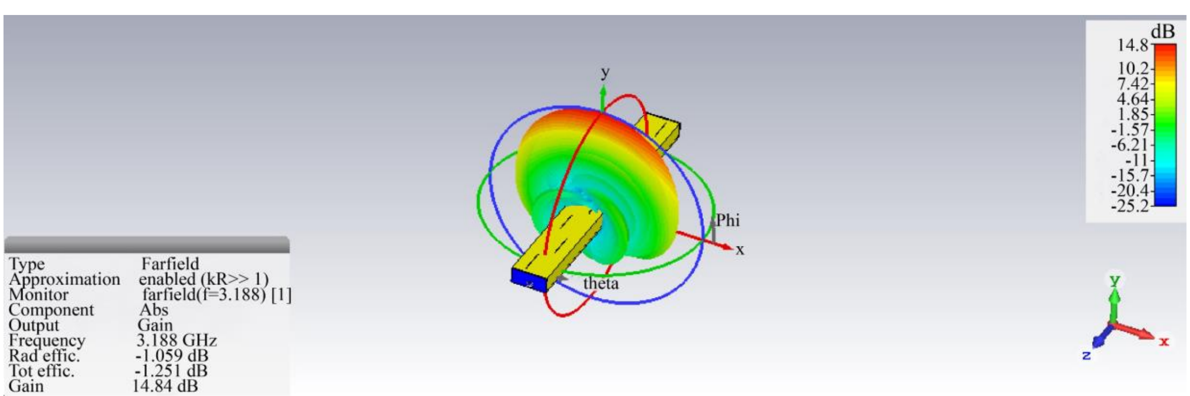
dB
14.8
10.2
7.42
4.64
1.85
-1.57
-6.21
-11
-15.7
-20.4
-25.2
y
Phi
x
theta
Type Farfield
Approximation enabled (kR>> 1)
Monitor farfield(f=3.188) [1]
Component Abs
Output Gain
Frequency 3.188 GHz
Rad effic. -1.059 dB
Tot effic. -1.251 dB
Gain 14.84 dB

(e)

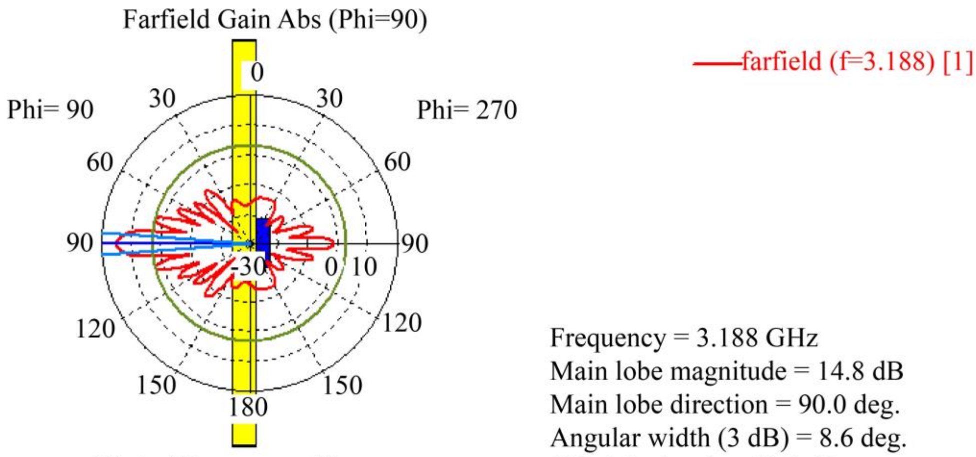

(f)

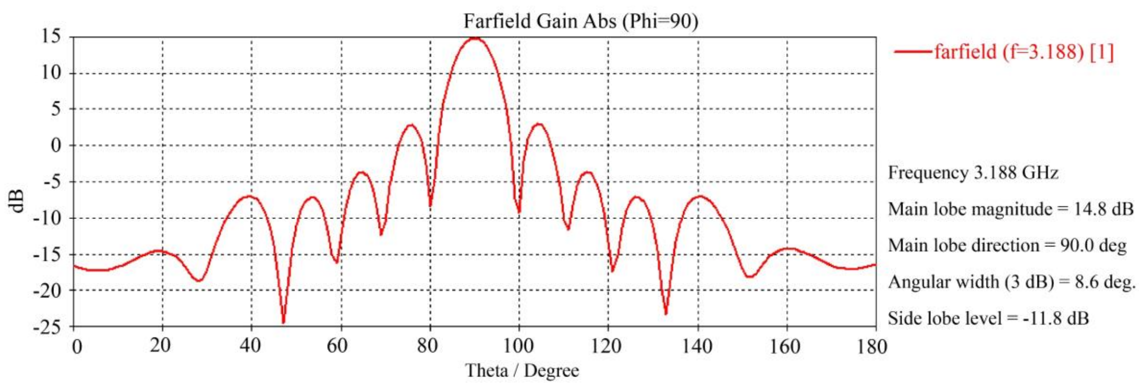

(g)

Fig. 8 8SWG (a) Design, (b) S11 plot, (c) VSWR plot, (d) E-field distribution, (e) Far-field, (f) Radiation pattern, and (g) Gain plot.

The design of an 8 SWG can be considered an extension of the 4 SWG. The dimensions of the WG and the slots are unchanged. However, the slots are 8 in number and arranged much more closely. However, following the same symmetry shown in Figure 8 (a), all the radiate slots are arranged or limited to only the secondary WG. The energy is coupled to the secondary radiating WG through a coupling slot of the primary WG.

The characteristics of the 8 SWG are studied in terms of several radiation parameters. More significantly, the resonant band of operation extends from 3.18 GHz to 3.2 GHz as shown in Figures 8(b) and 8(c), in which the corresponding S11 and VSWR are plotted. The corresponding band of frequencies' respective values will be below the desired benchmark values.

The field distribution plotted in Figure 8 (d) is useful in understanding the field concentration through the regions of the WG. It is evident from the plot that the concentration of field follows the same nature as that of cases 1 and 2.

Table 2. Comparing the radiation patterns and beamwidth in three different situations

S.No	Case	Beamwidth and radiation patterns
1	WG with single slot	The resonant frequency identified as 3.27 GHz with an excellent wideband feature
2	Four Slotted WG (4SWG)	The radiation is concentrated through one hemisphere, which provides a highly directional characteristic. The beam width and the main beam placement are read directly.
3	8-Slot Waveguide (8-SWG)	The beamwidth can be analyzed from the 2D rectangular gain plot given in Figure 5(g). The concession of the beamwidth can be clearly witnessed from the plot.

The 3D radiation plot given in Figure 8(e) can be used to release the directional features of the 8 SWG. The severity is evident from the 2D radiation pattern plot in Figure 8(f).

In either case, the radiation is concentrated on one hemisphere like the way in 4 SWG. The beamwidth can be analyzed from the 2D rectangular gain plot given in Figure 8(g). The concession of the beamwidth can be clearly witnessed from the plot.

Table 2 compares the results from three different scenarios.

A prototype of the suggested non-uniform array antenna has been constructed, and its characteristics have been evaluated. In light of the measurement's results, the SLL is better than -27 dBs, and the gain is 15 dB.

Applications: Improving ion Source Performance, generating radiation nulls, improving bandwidth, transferring energy between waveguides.

5. Conclusion

Waveguide slot array antennas have unique qualities that make them superior to microstrip antennas in terms of loss and simpler in terms of structure than reflector antennas. As a result, they are widely employed for high-gain flat antennas in wave wireless communication systems. 4-slotted and 8-slotted WG characteristics are successfully studied, designed, and simulated structures. The gain characteristics are significantly impacted along with the directivity and, subsequently, the beam width. The narrow down in the beamwidth due to a greater number of radiating slots is obvious and analogous to the concentration radiation, which usually takes place in an array with an increase in the number of elements.

Similarly, as the slots are oriented only on one surface, the corresponding radiation is also concentrated in one hemisphere due to the absence of radiation slots on the other side. The likely reason is attributed to fabrication flaws in the thin adhesive layers. One conceivable strategy to reduce this reflection difference is to adjust the lengths of the coupling slots, which will be tested in future work.

Acknowledgements

The author greatly acknowledges the Centurion University of Technology and its management for providing the necessary facilities to conduct this research.

References

[1] R. Elliott, "An Improved Design Procedure for Small Arrays of Shunt Slots," *IEEE Transactions on Antennas and Propagation*, vol. 31, no. 1, pp. 48-53, 1983. [CrossRef] [Google Scholar] [Publisher Link]

[2] R. Elliott, and W. O'Loughlin, "The Design of Slot Arrays Including Internal Mutual Coupling," *IEEE Transactions on Antennas and Propagation*, vol. 34, no. 9, pp. 1149-1154, 1986. [CrossRef] [Google Scholar] [Publisher Link]

[3] G. Mazzarella, and G. Panariello, "Evaluation of Edge Effects in Slot Arrays Using the Geometrical Theory of Diffraction," *IEEE Transactions on Antennas and Propagation*, vol. 37, no. 3, pp. 392-395, 1989. [CrossRef] [Google Scholar] [Publisher Link]

[4] S.R. Rengarajan, and G.M. Shaw, "Accurate Characterization of Coupling Junctions in Waveguide-Fed Planar Slot Arrays," *IEEE Transactions on Microwave Theory and Techniques*, vol. 42, no. 12, pp. 2239-2248, 1994. [CrossRef] [Google Scholar] [Publisher Link]

[5] P.B. Katehi, "Dielectric-Covered Waveguide Longitudinal Slots with Finite Wall Thickness," *IEEE Transactions on Antennas and Propagation*, vol. 38, no. 7, pp. 1039-1045, 1990. [CrossRef] [Google Scholar] [Publisher Link]

[6] S.R. Rengarajan, "Compared Broad-Wall Slots for Array Applications," *IEEE Antennas and Propagation Magazine*, vol. 32, no. 6, pp. 20-26, 1990. [CrossRef] [Google Scholar] [Publisher Link]

[7] L. Josefsson, "Analysis of Longitudinal Slots in Rectangular Waveguides," *IEEE Transactions on Antennas and Propagation*, vol. 35, no. 12, pp. 1351-1357, 1987. [CrossRef] [Google Scholar] [Publisher Link]

[8] A. Oliner, "The Impedance Properties of Narrow Radiating Slots in the Broad face of Rectangular Waveguide: Part I--Theory," *IRE Transactions on Antennas and Propagation*, vol. 5, no. 1, pp. 4-11, 1957. [CrossRef] [Google Scholar] [Publisher Link]

[9] Fred Halsall, *Data Communications, Computer Networks, and Open Systems*, Addison-Wesley, pp. 1-907, 1996. [Google Scholar] [Publisher Link]

[10] Trevor Marshall, 802.11b WLAN Waveguide Antennas – Unidirectional and Omnidirectional, 2001. [Online]. Available: http://www.trevormarshall.com/waveguides.htm

[11] Una Perovic, "*Investigation of Rectangular, Uni-Directional, Horizontally Polarised Waveguide Antennas with Longitudinal Slotted Arrays Operating at 2.45GHz*," Theses, Wits University, pp. 1-12, 2006. [Google Scholar] [Publisher Link]

[12] C.T. Tai, *Characteristics of Linear Antenna Elements*, Antenna Engineering Handbook, McGraw-Hill, pp. 3-8, 1961. [Google Scholar]

[13] Lingkuan Meng et al., "Aspect Ratio Dependent Analytic Model and Application in Deep Silicon Etch," *ECS Solid State Letters*, vol. 3, no. 5, pp. 1-4, 2014. [CrossRef] [Google Scholar] [Publisher Link]

[14] Alejandro Sánchez-Postigo et al., "Suspended Germanium Waveguides with Subwavelength-Grating Metamaterial Cladding for the Mid-Infrared Band," *Optics Express*, vol. 29, no. 11, pp. 16867-16878, 2021. [CrossRef] [Google Scholar] [Publisher Link]